A Quantitative Approach to Screen for Nephrotoxic Compounds *In Vitro*

Melanie Adler,*[†] Susanne Ramm,* Marc Hafner,* Jeremy L. Muhlich,* Esther Maria Gottwald,[†] Elijah Weber,[‡] Alenka Jaklic,[‡] Amrendra Kumar Ajay,[†] Daniel Svoboda,[§] Scott Auerbach,[∥] Edward J. Kelly,[‡] Jonathan Himmelfarb,[¶] and Vishal S. Vaidya*[†]**

*Laboratory of Systems Pharmacology, Harvard Program in Therapeutic Sciences, Harvard Medical School, Boston, Massachusetts; [†]Renal Division, Department of Medicine, Brigham and Women's Hospital, Boston, Massachusetts; [‡]Department of Pharmaceutics, University of Washington, Seattle, Washington; [§]Social and Scientific Systems, Durham, North Carolina; [∥]National Toxicology Program, National Institute of Environmental Health Sciences, Research Triangle Park, North Carolina; [¶]Kidney Research Institute, Department of Medicine, University of Washington, Seattle, Washington; and **Department of Environmental Health, Harvard T.H. Chan School of Public Health, Boston, Massachusetts

ABSTRACT

Nephrotoxicity due to drugs and environmental chemicals accounts for significant patient mortality and morbidity, but there is no high throughput *in vitro* method for predictive nephrotoxicity assessment. We show that primary human proximal tubular epithelial cells (HPTECs) possess characteristics of differentiated epithelial cells rendering them desirable to use in such *in vitro* systems. To identify a reliable biomarker of nephrotoxicity, we conducted multiplexed gene expression profiling of HPTECs after exposure to six different concentrations of nine human nephrotoxicants. Only overexpression of the gene encoding heme oxygenase-1 (HO-1) significantly correlated with increasing dose for six of the compounds, and significant HO-1 protein deregulation was confirmed with each of the nine nephrotoxicants. Translatability of HO-1 increase across species and platforms was demonstrated by computationally mining two large rat toxicogenomic databases for kidney tubular toxicity and by observing a significant increase in HO-1 after toxicity using an *ex vivo* three-dimensional microphysiologic system (kidney-on-a-chip). The predictive potential of HO-1 was tested using an additional panel of 39 mechanistically distinct nephrotoxic compounds. Although HO-1 performed better (area under the curve receiver-operator characteristic curve [AUC-ROC]=0.89) than traditional endpoints of cell viability (AUC-ROC for ATP=0.78; AUC-ROC for cell count=0.88), the combination of HO-1 and cell count further improved the predictive ability (AUC-ROC=0.92). We also developed and optimized a homogenous time-resolved fluorescence assay to allow high throughput quantitative screening of nephrotoxic compounds using HO-1 as a sensitive biomarker. This cell-based approach may facilitate rapid assessment of potential nephrotoxic therapeutics and environmental chemicals.

Drugs and environmental chemicals, such as aminoglycoside antibiotics, analgesics, chemotherapeutic agents, and heavy metals, as well as endemic toxins like aristolochic acid are a common cause of AKI or CKD.[1,2] Current approaches to conduct safety and risk assessment of compounds rely predominantly on animal studies, and these results are extrapolated to dose effects in humans despite knowledge that the typical responses of animal models and humans can differ greatly.[3] The lack of adequate models to accurately predict human toxicity contributes to an underestimation of the

kidney toxic potential of new therapeutic candidates, which also explains why nephrotoxic effects in patients are often only detected during late phase

clinical trials or, in some cases, after regulatory approval.[4] Additionally, few registered chemicals have been fully assessed for their potential to cause kidney toxicity, while the number of new chemicals being synthesized annually for use in consumer products is increasing rapidly. Given the societal burden of kidney disease and the insensitivity of current methods to detect it, there is an urgent need to develop quantitative, sensitive, and robust methods for predictive assessment of human kidney toxicity.

Advancing early-stage safety assessment of large numbers of compounds, a paradigm shift in toxicology initiated by the Tox21 program, demands moving away from whole animal testing toward less expensive and higher throughput cell-based assays.[5,6] Currently, there is no *in vitro* method that can be used in a high throughput manner to identify kidney toxic agents early in the process before reaching humans. Immortalized kidney epithelial cell lines, derived from human kidney (HK-2),[7] pig kidney (LLC-PK1), or dog kidney (MDCK),[8] frequently used for nephrotoxicity studies, do not fully express all the differentiated functions found in their *in vivo* counterparts due to loss of polar architecture and changes in drug transporter expression.[9,10] Primary proximal tubular epithelial cells of human origin, being the predominant target of most toxicants in the kidney,[11] are characterized by polarity and junctional assembly of epithelia, brush border enzyme activity, and metabolic and transport capacity.[10,12–14] Among the currently available two-dimensional (2D) models, they are the model that comes closest to the ideal with respect to kidney physiology and toxicology studies.

The primary objective of this study was to develop a cell-based approach for safety screening of kidney toxic compounds. Specifically the aims were: to evaluate the structural and functional characteristics of human primary tubular epithelial cells; to identify a translational biomarker that, either alone or in combination with known markers, would enable prediction of risk for kidney toxicity across species and platforms; and to develop a time resolved fluorescence resonance energy transfer (FRET) assay for measuring the biomarker, which would allow improved quantitation of kidney toxicity in a high throughput manner.

RESULTS

Structural and Functional Characterization of Primary HPTECs as a Suitable *In Vitro* Model for Screening Kidney Toxicity

We structurally and functionally characterized human proximal tubular epithelial cells (HPTECs) to determine whether they exhibit features of a differentiated kidney proximal tubular epithelium. HPTECs expressed zonula occludens 1, cytokeratin 18 (CK18), E-cadherin, and N-cadherin, indicating tight junction assembly and cell polarity (Figure 1A). The cells also showed a consistent expression of kidney-specific cadherin, as well as a wide range of efflux and influx

transporters, such as megalin, aquaporin-1, multidrug resistance protein 2 (MRP2), P-glycoprotein (MDR1), and organic cation transporter 2 across different passages and cultivation periods (Figure 1B). These findings correlated well with the RNA expression pattern observed in human kidney (Figure 1B). In contrast, aquaporin-1 and kidney-specific cadherin mRNA were not detected in HK-2 cells, which are immortalized human proximal tubular cells. The development of HPTECs to polarized confluent monolayers on collagen IV coated transwells was evaluated by an increase in transepithelial electrical resistance over 7 d of culture (Figure 1C). Confluent monolayers of HPTECs in well plates also formed typical domes, indicative of transepithelial solute transport (data not shown). Sucrose transport was demonstrated to be active across cell monolayers grown on transwell filters for 7 d as well as in monolayers cultured in well plates (Figure 1D). Based on a significant cellular efflux of rhodamine 123, a fluorescent MDR1 substrate, we showed that the transporter is functional in HPTECs (Figure 1E). Time and dose-dependent glucose transport (Figure 1F, left panel) could be attributed to Na^+-dependent (SGLT) and Na^+-independent (GLUT) transport processes (Figure 1F, right panel). Exposure of cells to various concentrations of cadmium chloride ($CdCl_2$) for up to 24 h increased γ-glutamyl-transferase activity and elevated levels of cellular glutathione in a time and dose-dependent manner (Figure 1G). Finally, activity and functionality of mitochondria in HPTECs were demonstrated after treatment with different inhibitors of oxidative phosphorylation, causing either loss of mitochondrial membrane potential (MMP) without production of reactive oxygen species (ROS) (carbonyl cyanide m-chlorophenyl hydrazone), or pronounced production of ROS without affecting the MMP (oligomycin A) (Figure 1H). These data suggest that HPTECs represent a suitable *in vitro* model as they retain many of the phenotypic as well as functional characteristics of the human proximal tubule.

Identification of HO-1 as a Biomarker for *In Vitro* Kidney Toxicity

In order to identify a potential biomarker that allows identification of kidney toxic compounds before changes in cell morphology or detectable loss of viability occur, we conducted gene expression profiling by measuring 1000 landmark genes characteristic of the variability of the transcriptome.[15] HPTECs were cultured for 3 d in collagen-coated multiwell plates until confluence before treatment with a discovery panel (Supplemental Table 1) consisting of nine structurally and mechanistically distinct kidney toxic compounds (cisplatin, cyclosporin A (CsA), cadmium chloride ($CdCl_2$), aristolochic acid (AA), gentamicin, FK-506, tobramycin, doxorubicin, ochratoxin A) versus the nontoxic compound (carboplatin) at concentrations ranging from 1.6 μM to 20 mM over four different time points (3, 6, 12 and 24 h). Supplemental Figure 1 shows compound-induced changes in phenotype of the cells and loss of cell viability based on ATP concentrations. The
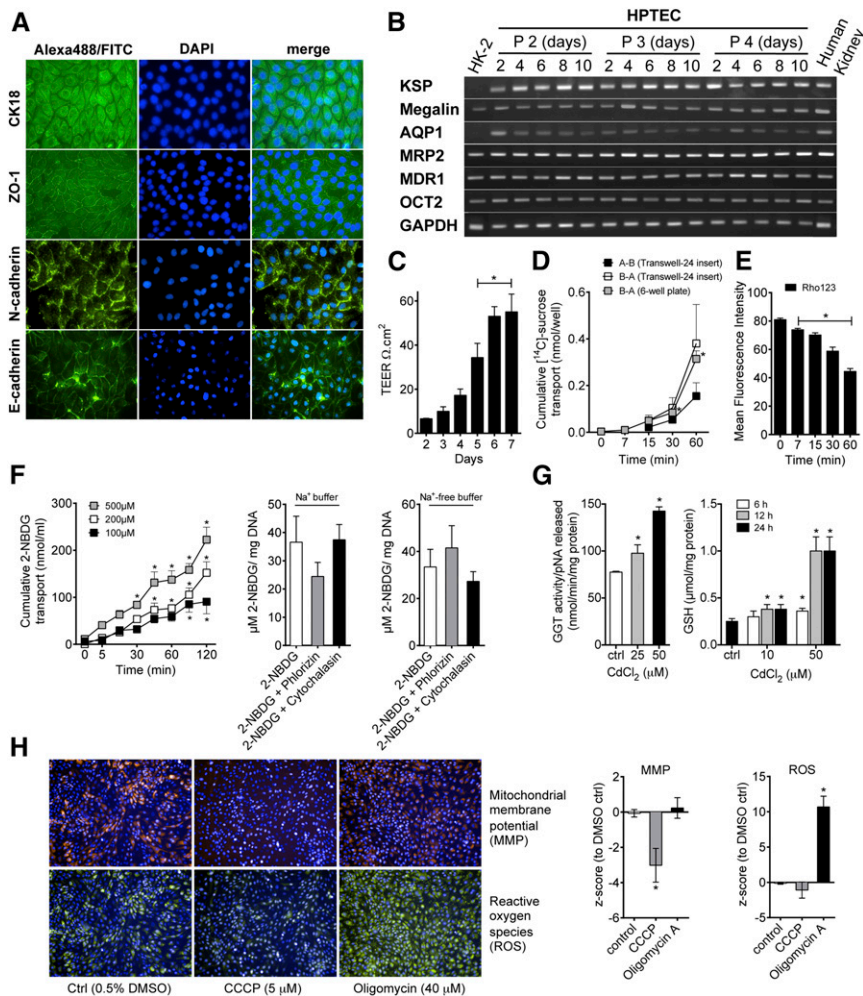
Figure 1. Human proximal tubular epithelial cells (HPTECs) demonstrate a well-defined differentiated phenotype resembling human proximal tubule kidney cells. (A) Immunohistochemical staining (green) of a representative cell monolayer, seeded on glass slides, shows expression of cytokeratin 18, zonula occludens-1, N-cadherin and E-cadherin proteins (Original magnification, ×40). DAPI was used to counterstain nuclei and is merged with indicated immunofluorescence staining. (B) Semiquantitative PCR gel for proximal tubule-specific genes such as kidney-specific cadherin (356 bp), megalin (296 bp), aquaporin-1 (365 bp), MRP2 (356 bp), MDR1 (251 bp), organic cation transporter 2 (217 bp). Glyceraldehyde-3-phosphate dehydrogenase was used as a loading control (GAPDH, 197 bp). PCR was performed on RNA isolated from HPTECs grown on 12-well plates in two independent experiments cultured up to 10 d and four different passages. RNA from HK2 cells and human kidney were used as comparators. (C) Cells develop a transepithelial electrical resistance (TEER) when cultured on transwell-24 support with an initial density of 25,000 cells/filter. TEER increases to a maximum of $55.07 \pm 2.7\Omega$ cm^2 in 7 d. (D) Cumulative uptake of [^{14}C]-sucrose via the apical (A) to basolateral (B) or B to A directions was measured after 7, 15, 30, and 60 min. Similar B–A sucrose flux was observed in cells grown on transwell filters and well plate. (E) Rhodamine 123 (Rho123), a fluorescent dye, was used to measure MDR1 activity. The significant decrease in Rho123 fluorescence was determined after incubation with 0.5 μg/ml for 2 h by flow cytometry over a period of 60 min. (F) Cells show dose and time-dependent uptake of a fluorescent glucose substrate (2-NBDG) and inhibition assays suggest activity of Na$^+$-dependent glucose transport (SGLT inhibition with phlorizin) as well as Na$^+$-independent (GLUT inhibition with cytochalasin B). (G) Effect of cadmium chloride on the γ-glutamyl transferase (GGT) activity and glutathione (GSH) levels in HPTECs. (H) Activity and functionality

1000 selected transcripts were measured for each sample in a single well of a 384-well plate using Luminex based technology.[15] For each gene and drug, we calculated the correlation between the dose and the fold change in gene expression at each time point and calculated an empirical *P* value (Figure 2, A and B, see the methods section for details). Based on all gene-drug pairs, we found that HMOX1 (HO-1, heme oxygenase-1) was the only gene whose overexpression significantly correlated (false discovery rate (FDR) <0.01) with increasing dose for six of the nine compounds, including AA, CdCl$_2$, CsA, cisplatin, gentamicin, and FK-506 (Figure 2C). There was no significant increase in HO-1 mRNA expression in response to ochratoxin A, tobramycin, doxorubicin, and the nontoxic compound carboplatin. In addition to HO-1, some apoptotic genes such as GADD45A and PMAIP1, were also upregulated in five of the nine compounds as a consequence of a late toxic effect, indicating decreased cell viability (Figure 2C, Supplemental Figure 1). HO-1 mRNA and protein upregulation was further confirmed using quantitative RT-PCR, ELISA and immunofluorescence (Figure 3A). HO-1 protein levels were significantly increased in a dose-dependent manner following exposure to cisplatin, CsA, CdCl$_2$, AA, gentamicin, tobramycin, and FK-506 for 24 h (Figure 3A), whereas the highest concentration of some compounds resulted in a temporal response of HO-1 as early as 3 h (Supplemental Figure 2A). HO-1 increase was not directly correlated to an increase in production of ROS, showing that it can also detect compounds whose mechanism of toxicity does not involve oxidative stress (Figure 3B). HO-1 mRNA levels were also found to be upregulated more than 10-fold in human proximal renal tubular epithelial cells purchased from

of mitochondria in HPTECs is shown after perturbation with carbonyl cyanide m-chlorophenyl hydrazone (CCCP) (decreases MMP without induction of ROS), and oligomycin A (induces ROS without loss of MMP). Data corresponds to the mean±SEM from three independent experiments performed in triplicate (*P<0.05 compared with control).
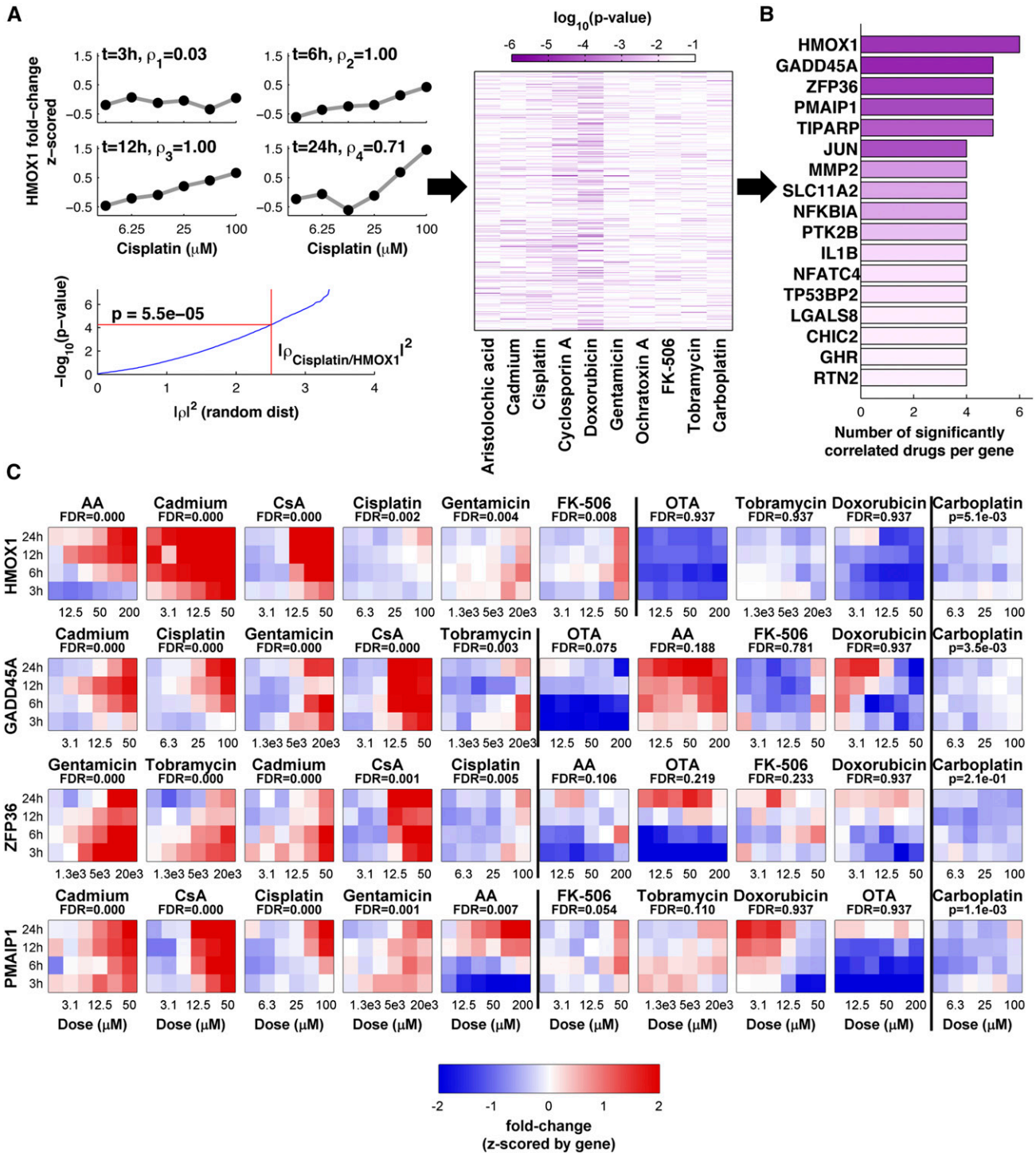
Figure 2. HMOX1 differential expression is positively correlated with doses across the highest number of compounds. High throughput gene expression profiling based on the measurement of 1000 genes was performed in human proximal tubular epithelial cells (HPTECs) exposed to a discovery panel of 10 compounds in six different concentrations for 3, 6, 12, and 24 h. (A) For each time point, we calculated the Spearman's correlation between the six doses and the fold change in mRNA for each gene. A representative example is shown for HMOX1 and cisplatin. The sum of square of the four correlation values is compared with the distribution of values with random data to yield a P value for each pair of gene and compound. Results are shown in a heat map. (B) Based on a cutoff of false discovery rate of 0.05, we ordered genes based on the number of compounds for which gene expression is significantly correlated with dose. HMOX1 is identified as the top gene showing a dose-dependent correlation in six of the nine toxic compounds. Color intensity reflects the average P value for significantly correlated toxicants (the darker, the more significant). (C) Dose and time dependent fold change of
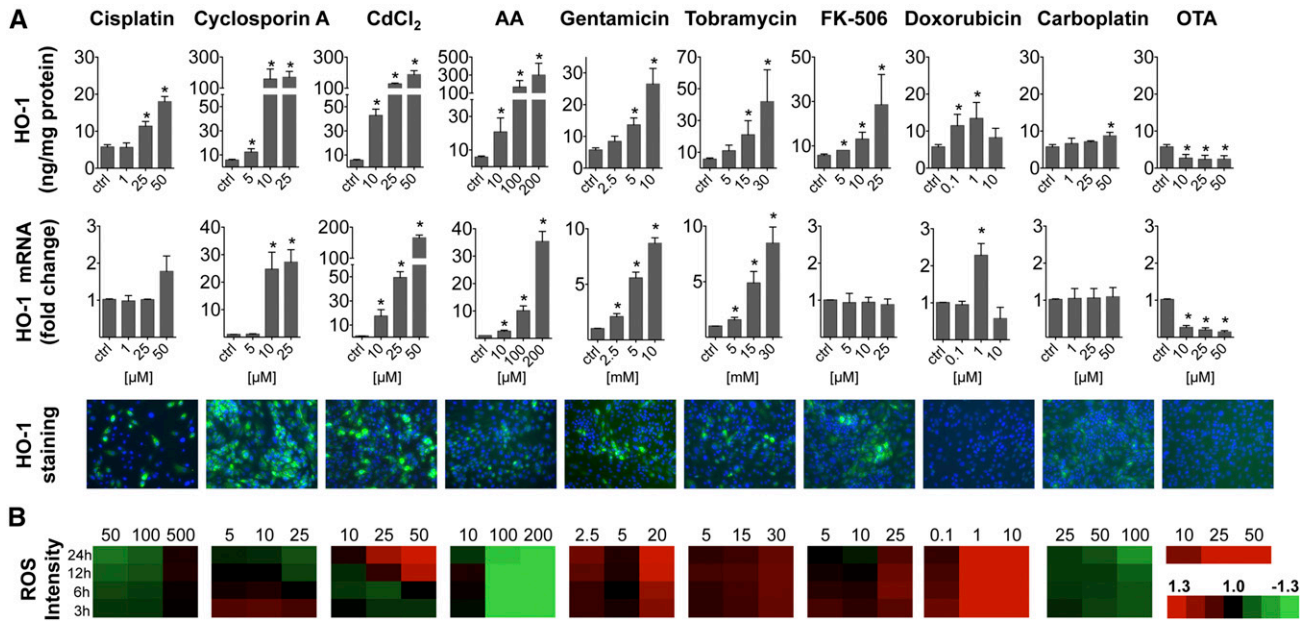
Figure 3. Induction of HO-1 protein in response to nephrotoxic compounds correlates with mRNA expression in human proximal tubular epithelial cells (HPTECs). (A) Changes of HO-1 at mRNA and protein levels measured by ELISA, quantitative RT-PCR, and immunostaining in HPTECs after incubation with model compounds of the discovery panel for 24 h. HO-1 protein and mRNA expression was measured in cell lysates of HPTECs cultured and treated in 6-well plates in triplicate in three independent experiments. Results are presented as mean±SEM (n=3). *P<0.05. Staining of HO-1 (green) was performed in cells seeded on 8-well collagen-coated glass-well chamber slides (Original magnification, ×40). Representative images are shown for the highest concentration of each compound. (B) Modulation of cellular HO-1 does not exclusively correlate with increase in ROS. ROS was quantified using CellROX dye and fluorescence intensity was calculated as fold change compared with 0.5% DMSO control.

two different sources (LONZA and ATCC) (Supplemental Figure 2B). Incubation of conventionally used immortalized human kidney cell line (HK-2) with similar concentrations of cisplatin, $CdCl_2$, and AA also showed an increase of HO-1 protein levels; however, gentamicin failed to induce an upregulation of HO-1, and carboplatin (nontoxic control) increased HO-1 concentrations, representing a false positive result (Supplemental Figure 2C).

Translatability of HO-1 as a Biomarker across Species and Platforms
The relevance of HO-1 induction in *in vivo* models of kidney toxicity was assessed computationally by mining two large toxicogenomic databases for HO-1 expression following kidney tubular toxicity. The National Toxicology Program's DrugMatrix as well as the National Institute of Biomedical Innovation's Toxicogenomics Project-Genomics Assisted Toxicity Evaluation System (TG-GATES) are the two largest toxicogenomics databases and analysis tools that contain *in vivo*

multi-organ rat toxicogenomic data for more than 700 chemicals that are integrated with histopathology and clinical chemistry results from the same animals. As expected,[16] Havcr1 (Kim-1) increase (approximately 47-fold, DrugMatrix P=2.14E-29, TG-GATES P=2.12E-11) was strongly associated with kidney tubular necrosis in both the DrugMatrix and TG-GATES kidney datasets (Figure 4A, Supplemental Material). *Hmox1* was present in both the databases and was upregulated (approximately 2-fold, DrugMatrix P=3.11E-11, TG-GATES P=3.53E-3) with kidney tubular necrosis and kidney tubular regeneration (Figure 4A, Supplemental Material). Furthermore, *Hmox1* expression in both the DrugMatrix and TG-GATES dataset was positively correlated (using linear regression) with expression of a number of transcriptionally inducible biomarkers described in the literature as potential biomarkers of preclinical kidney toxicity (Table 1).

Translatability of HO-1 increase in cells from 2D systems to three-dimensional (3D) systems was assessed by using *ex vivo* 3D modular microphysiological system (MPS) with human

gene expression (z-scored for each gene) for the top four genes of across all 10 compounds. Compounds are ordered for each gene based on the P value of the correlation. A black line separates the compounds with significant correlations from the others, while carboplatin is shown on the right as it serves as a nontoxic control. In addition to HMOX1, an early stress response protein, genes associated with growth arrest and DNA damage (GADD45A), transcriptional regulation of TNF (ZFP36) and apoptosis (PMAIP1) were found to be significantly upregulated in five of nine compounds. Gene expression changes were calculated as mean compared with 0.1% DMSO controls (n=4).
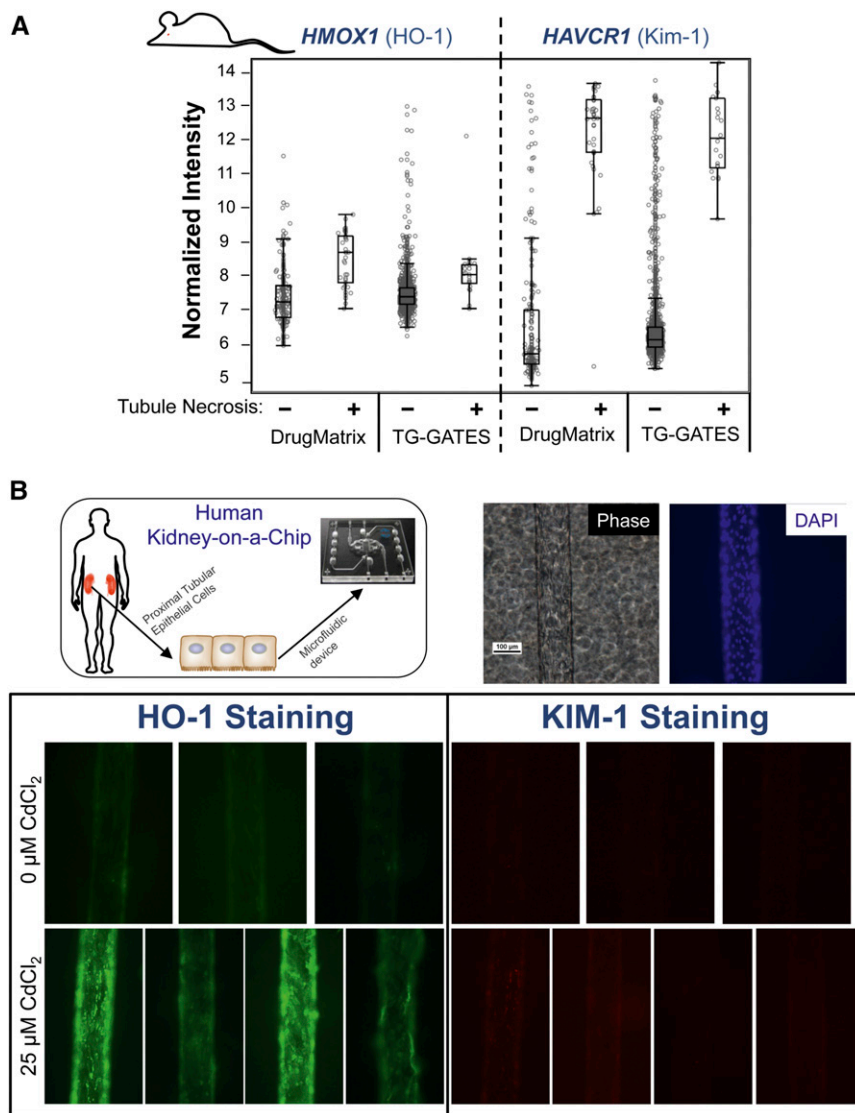
Figure 4. Increase of HO-1 expression in rats and 3D human kidney microfluidic systems following renal injury. (A) Normalized expression intensity of HMOX1 and HAVCR1 in samples positive (+) for tubular necrosis is higher than samples negative (–) for tubule necrosis in the *in vivo* toxicogenomic databases (DrugMatrix and Toxicogenomics Project-Genomics Assisted Toxicity Evaluation System (TG-GATES)). Each data point represents intensity for a given sample. The bounding box extends from the first to third quartiles, with the central bar indicating the median intensity. Whiskers extend from the ends of the box to the outermost data point that falls within the third quartile+1.5× (interquartile range) and first quartile–1.5×(interquartile range), or to the end of the range. Data points are jittered. (B) Schematic diagram depicting concept of human kidney-on-a-chip. Human proximal tubule epithelial cells (HPTECs) form a confluent tubule in the chip as depicted by the phase contrast of cells and DAPI fluorescent imaging of nuclei. Exposure of HPTECs in the chips with 25 μM CdCl$_2$ for 48 h resulted in an upregulation of HO-1 depicted by the FITC fluorescent stain. Control devices showed minimal expression of HO-1. KIM-1 expression, absent in untreated devices, marginally increased in response to cadmium chloride in two of four devices.

kidney proximal tubule derived epithelial cells (Figure 4B). HPTECs self-assemble and recapitulate an *in vivo* structure and function within the microfluidic chips.[17] Under normal conditions, HPTECs in chips show little to no expression of biomarkers, KIM-1 and HO-1, reflecting absence of injury. Consistent with the results obtained using a 2D system (Figure 3) an extremely robust induction of HO-1 was observed in comparison to a modest increase in KIM-1 after exposure of 25 μM cadmium chloride for 48 h (Figure 4B). Plasma and urinary levels of HO-1 have been shown to be a biomarker for AKI in humans[18] and here we present evidence that HO-1 expression was significantly upregulated in primary HPTECs, as well as in rat kidneys and the 3D human kidney-on-a-chip system following tubular toxicity, thereby extending the relevance of HO-1 as a translational biomarker. In comparison, biomarkers like KIM-1 that have very high sensitivity and specificity to detect kidney toxicity in rodents[16] do not show a consistent upregulation following injury to the human primary proximal tubular epithelial cells (Figure 4B, Supplemental Figure 3).

Potential of HO-1 to Predict Kidney Toxicity *In Vitro*

In order to further evaluate the robustness and sensitivity of HO-1, we tested an additional validation panel (Supplemental Table 1) of 39 well characterized mechanistically distinct compounds that included nontoxic compounds as well as known human kidney toxicants, acting either by direct proximal tubule toxicity or via secondary mechanisms, such as crystal formation in the tubules. All compounds were analyzed for their ability to significantly alter: the number of total cells; the concentration of ATP in cells; the number of dead cells; and the HO-1 concentration in cells. Plotting the maximal significant deregulation compared with control that could be observed at any given concentration of a drug, we calculated the area under the curve receiver-operator characteristic curve (AUC-ROC) for each of the four assays. Including all nontoxic compounds and compounds directly toxic to the proximal tubule, HO-1 was associated with a similar but slightly higher AUC-ROC (0.89) compared with the three other assays: cell number (0.88), cell viability (0.78) and dead cells (0.86) (Figure 5, A and B). This held true, irrespective of whether nephrotoxicants following secondary mechanisms of toxicity were included in the analyses or not

Table 1. Correlation (*R*) between normalized intensity of genes across all probe sets exhibiting significant coexpression with *HMOX1*, for DrugMatrix and TG-GATES datasets

Gene Symbol	DrugMatrix		TG-GATES	
	Correlation (*R*)	Significance (*P* Value)	Correlation (*R*)	Significance (*P* Value)
Tissue inhibitor of metalloproteinase 1 (Timp1)	0.44	6.25E-69	0.28	2.18E-26
Secreted phosphoprotein 1 (Spp1)	0.21	1.48E-16	0.17	4.11E-11
Clusterin (Clu)	0.29	7.03E-29	0.12	7.25E-06
Alpha-2-macroglobulin (A2m)	0.29	5.26E-29	0.09	0.0005
Lipocalin (Lcn2)	0.43	1.08E-65	0.25	4.40E-22
Fibronogen β (Fgb)	0.42	2.69E-63	0.18	6.33E-12
Laminin, gamma 2 (Lamc2)	0.37	2.23E-48	0.25	2.40E-21
Cd44	0.40	4.89E-57	0.16	3.32E-09
Hepatitis A virus cellular receptor 1 (Havcr1) also called KIM-1	0.49	9.98E-87	0.3	4.98E-30

(Figure 5B). The performance of HO-1 as a biomarker was more sensitive (75%) compared with other known assays of cell death/viability (Figure 5B). The predictive performance of HO-1 in combination with cell number (chi-squared $P<0.001$), number of dead cells ($P<0.001$), or ATP ($P<0.001$) significantly improved as compared with individual assays (Figure 5C). Furthermore, HO-1 plus cell number outperformed the other combinations when examining proximal tubule toxic compounds (AUC-ROC=0.92) as well as after integrating toxicants with secondary mechanisms (AUC-ROC=0.83). The sensitivity of HO-1 as a single biomarker could be increased from 75% to 79% when combined with either cell number or the amount of dead cells (Figure 5C).

To also include the dose-response relationship for the assays that performed best, we computed the IC_{25} (concentration that reduces the number of cells by 25%), and used the HO-1 fold-change data to compute C_{HO-1} (concentration at which HO-1 expression was 2 SD away from baseline in the log domain). Normalized viability and HO-1 fold-change curves and computed IC_{25}/C_{HO-1} values for all compounds from the validation panel are shown in Supplemental Figure 4. Grouping of compounds in their response categories (Figure 5D) generally recapitulated the sensitivity and specificity obtained with the highest deregulation approach: 100% of nontoxic and 100% of secondary toxic compounds were −TOX/-HO-1, 80% of proximal tubule toxic compounds were either −TOX/+HO-1 or +TOX/+HO-1, demonstrating that HO-1 is even more sensitive when used in a dose-response manner. Additionally, for nearly all of the +TOX/+HO-1 compounds the C_{HO-1} was at least an order of magnitude lower than the IC_{25} (Figure 5E, Supplemental Figure 4), suggesting that toxicity-related changes in HO-1 expression occurred at a concentration below that at which cytotoxic effects can be detected. This finding strongly supports the use of HO-1 as a suitable *in vitro* biomarker for prediction of kidney toxicity.

Development and Optimization of a High Throughput Assay for Measurement of HO-1

Our next goal was to develop a high throughput assay to quantify HO-1 in a rapid and cost-efficient manner. We established a fast and simple assay that is based on a time resolved FRET between two epitopically distinct antihuman HO-1 antibodies that are labeled either with europium cryptate as the donor fluorochrome or d2 as the acceptor fluorochrome (Figure 6A). Antibodies were optimized to show a high fluorescence signal and differences between the background, negative (untreated cells) and positive (gentamicin, $CdCl_2$, HO-1 recombinant protein) controls (Figure 6, B and C). The final FRET signal increased significantly following gentamicin and $CdCl_2$ exposure and was not only significantly higher than DMSO or medium treatment but also 12–20-fold higher in both groups compared with the background. The homogeneous time resolved fluorescence (HTRF) assay was first evaluated and optimized by measuring HO-1 in cell lysates of HPTECs treated with the 10 compounds included in the discovery panel (Supplemental Table 1) in 96-well plates using both traditional ELISA and HTRF. A Spearman's correlation of 0.96 ($P<10^{-16}$) was observed between the two assays (Figure 6D). HO-1 was then quantified in cells cultured in 384 wells and treated with the 39 compounds of the validation panel (Supplemental Table 1), whereby the HO-1 levels obtained from the HTRF assay in response to most of the compounds, such as 4-aminophenol, amphotericin B, arsenic trioxide, citrinin, lead (II) acetate, omeprazole, rapamycin, rifampin, and tetracycline correlated well with immunofluorescence (Spearman's Rho=0.62, $P<10^{-15}$, Figure 6E, Supplemental Figure 5). In contrast to immunofluorescence, lack of sensitive methods to determine protein concentrations from cells cultured in mid or high throughput well-plate does not allow a normalization of the results from the HTRF to the protein content. Therefore, we observed a loss of range in HO-1 expression after treatment with 4-N-nonylphenol, doxorubicin, idarubicin, potassium dichromate, and puromycin dihydrochloride especially at higher concentrations showing >80% decrease in the cell viability. Apart from this limitation, this assay is a rapid way to quantify HO-1 in a high throughput manner.

DISCUSSION

One of the major challenges in developing safe and effective agents is the accurate prediction of human toxicity for new drug

A (ROC curves: Cell no., ATP, Dead cells, HO-1; PT toxic black line, Sec. toxic gray line; Sensitivity % vs 100 − Specificity %)

B

	Cell no.	ATP	Dead cells	HO-1
AUC-ROC	0.875 (0.780)	0.780 (0.675)	0.857 (0.756)	0.885 (0.802)
max YI	0.708 (0.613)	0.417 (0.391)	0.708 (0.613)	0.750 (0.581)
Cutoff	< 0.755	< 0.855	> 1.515	> 2.695
Sens./ Spec.	70.8/ 100	54.2/ 87.5	70.8/ 100	75.0/ 100
PPV/ NPV	1.000/ 0.533	0.929/ 0.389	1.000/ 0.533	1.000/ 0.571
Chi-square	12.09	4.233	12.09	13.71
P-value	0.0005	0.0396	0.0005	0.0002

C

	HO-1 + Cell no.	HO-1 + ATP	HO-1 + Dead cells
Chi-square	18.68	15.51	18.71
P-value	0.0001	0.0004	0.0001
Intercept (α_0)	3.455	-0.252	-2.757
Var.1 (α_1)	1.106	1.284	1.103
Var.2 (α_2)	-6.921	-2.419	0.744
AUC-ROC	0.922 (0.831)	0.901 (0.827)	0.901 (0.722)
Sens./ Spec.	79.2/ 100	67.7/ 87.5	79.2/ 100

D (bar chart: Count vs Classification; −TOX −HO-1, +TOX +HO-1, −TOX +HO-1, +TOX −HO-1)

E (scatter plot: HO-1 induction (μM) vs IC25 (μM); legend: Non-toxic, Nephrotoxic, Secondary toxic, HO-1 inducer)
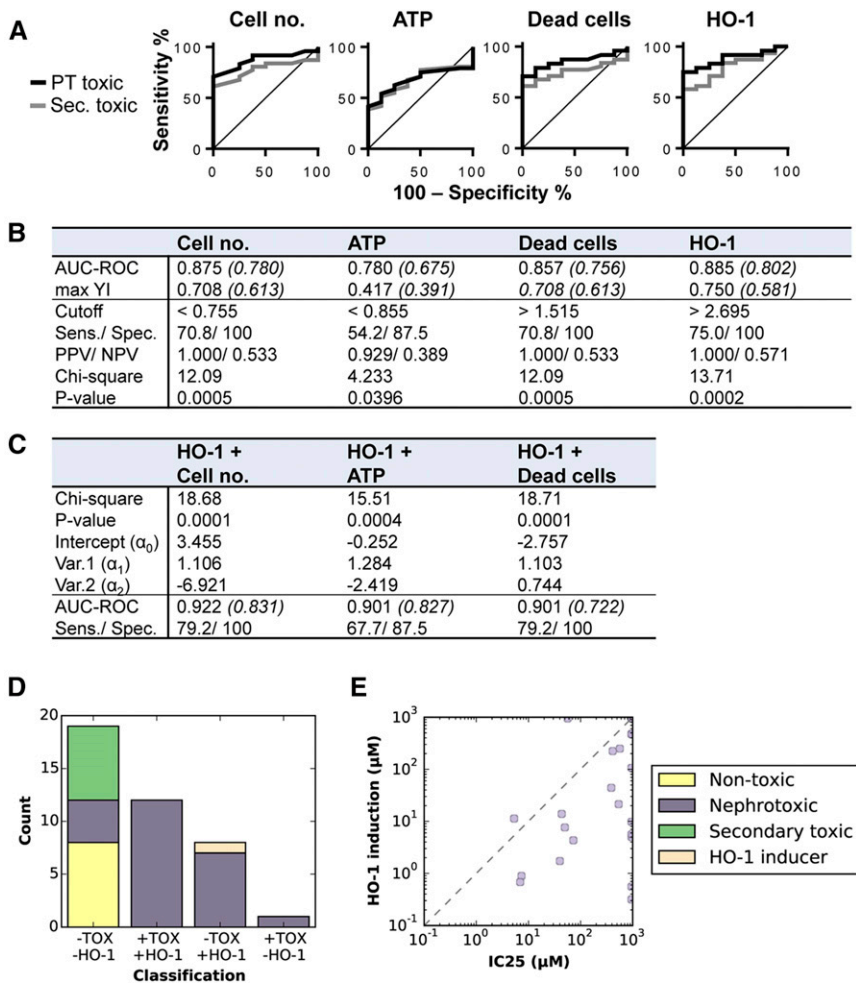
Figure 5. Comparison of HO-1 as biomarker for kidney injury with known cell viability/ cell death assays. Predictive value of four different assays (cell number [DAPI nuclear stain], ATP concentration [CellTiter Glo], dead cell number [TOTO-3 stain], and HO-1 concentration [immunofluorescence stain]) across 39 compounds of the validation panel (eight non-nephrotoxic, 24 directly nephrotoxic (proximal tubule (PT)), and seven indirectly nephrotoxic (via secondary mechanisms)). (A) Receiver-operator characteristic curves computed either just for PT toxic drugs (black line) or also including indirect nephrotoxicants (gray line). (B) Table displays area under the curve receiver-operator characteristic curves (AUC-ROC) both for PT toxic drugs only and when indirect nephrotoxicants are included (in brackets). Maximal Youden index is calculated as sensitivity (%)+specificity (%)−100 and was used to determine the optimal cutoff point for each assay where sensitivity and specificity are maximal. Applying this cutoff, sensitivity was calculated by dividing the number of true positive toxicants (TP) by the number of total toxicants in the validation panel. Specificity was calculated by dividing the number of true negative nontoxicants (TN) by the number of total nontoxicants in the set. The positive predictive value is defined as the ratio of TP to all compounds identified as toxic and the negative predictive value is calculated as the ratio of TN to all compounds identified as nontoxic. Chi-squared test statistic and corresponding *P* value describe the goodness of fit of the observed distribution (measured results in the respective assays) to the theoretical one (toxic or nontoxic). (C) Improvement of pre-dictivity via combination of cell death/viability assays with HO-1 was calculated using logistic regression. A combined output was calculated as $\alpha_0+\alpha_1$*value assay 1(HO-1) $+\alpha_2$*value assay 2. The final AUC-ROC were calculated using the combined output values both for PT toxic drugs only and when indirect nephrotoxicants are included (in brackets). (D) Assay response category (based on dose-response curves of HO-1 fold change and cell number) versus clinical toxicity classification. Each bar represents one assay response category; the colored segments correspond to clinical toxicity classes. Curcumin, a known nontoxic HO-1 inducer, is included for reference. (E) Scatter plot of C_{HO-1} (drug concentration at significant HO-1 induction) versus IC25 (drug concentration at 25% decrease in cell number). Observe that most drugs show significant HO-1 induction at a concentration an order of magnitude or more below the IC25. Each compound was tested in eight concentrations, starting from 0.1 μM to 554 μM for 24 h (*n*=4).

candidates and industrial chemicals.[19] An ideal cell culture system for drug screening would incorporate the two most fundamental properties of an *in vitro* approach: characteristics of the cells with respect to mimicking human physiology; and sensitivity, specificity, and robustness of a biomarker to quantitate toxicity. Although some clinically relevant *in vivo* kidney injury biomarkers (KIM-1 and NGAL) are expressed in some proximal tubule lines, their translation to cell-based screening assays has not yet been reported.[20] We did not observe KIM-1 upregulation in HPTECs cultured in 2D consistent with a previous study,[10] or even consistently when HPTECs were cultured in the microphysiological 3D kidney system (Figure 4B), highlighting the need for new biomarkers applicable to *in vitro* as well as *in vivo* and human studies. We addressed this issue in the current study and report three important advances: (*1*) HPTECs possess characteristics of differentiated epithelial cells, such as polar architecture, junctional assembly, expression and activity of transporters, ability to synthesize enzymes like glutathione and γ-glutamyl transferase thereby making them desirable to use in *in vitro* systems. (*2*) Changes in expression of HO-1 were found to be more sensitive in predicting compound toxicity in HPTECs than currently used assays of cell viability and cell death. In addition, we show that the sensitivity and specificity can be improved even further by combining the readout for HO-1 concentration and the total cell number, measured in the same well. (*3*) A newly developed HTRF
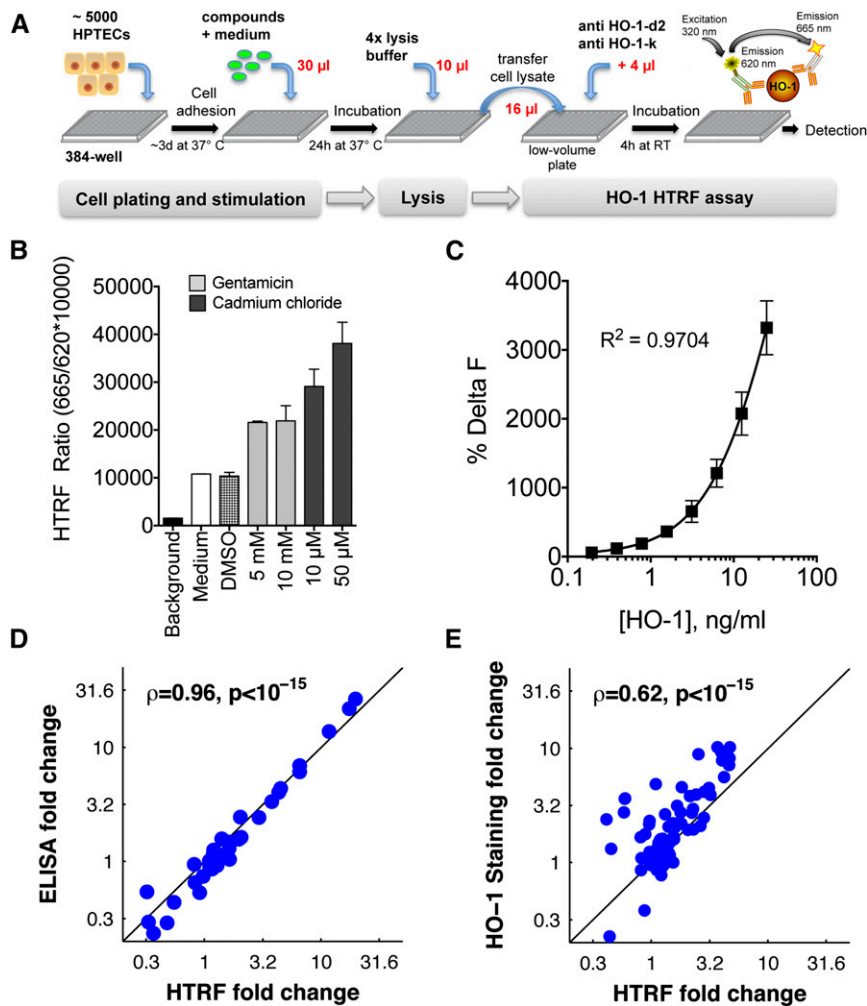
Figure 6. Development and evaluation of an homogeneous time resolved fluorescence (HTRF) assay for quantification of HO-1 in a high throughput manner. (A) Scheme of the experimental procedure of HO-1 HTRF assay performed in 384-well plate. When the acceptor labeled antihuman HO-1 antibody and the donor labeled antibody bind to HO-1, the two dyes are brought into close proximity with each other. Excitation of the donor with a light source triggers a fluorescence resonance energy transfer (FRET) toward the acceptor and the emission fluorescence (665 nm) can be detected after incubation for 4 h. This signal is proportional to the amount of human HO-1 present in the cell lysate. (B) Assay optimization based on the signal readout included best antibody pair analysis, serial dilution of the antibodies, time-dependent FRET signal development, cell number, and conditions for lysis of human proximal tubule epithelial cells (HPTECs) using several lysate buffers. Optimized assay revealed a robust signal difference between background, negatives (medium, DMSO) and positives (gentamicin, cadmium chloride). (C) Detection of recombinant human HO-1 protein verified that the HTRF assay results are reproducible. Data are presented from eight independent experiments, measured in duplicate (mean±SD, $n=8$). Delta F (%) is calculated by the following formula: sample-ratio–ratio background/ratio background). (D, E) Correlation between ELISA versus HTRF, and immunofluorescence versus HTRF performed in different assay formats. (D) Fold change of HO-1 was measured in lysates of HPTECs incubated with 10 compounds in 96-well plates after 24 h (see used concentrations in Figure 3; triplicate per experiment, $n=3$). (E) HO-1 response was quantified in HPTECs treated with 39 compounds in four concentrations starting from 554 μM (10-fold dilution) in 384-well plate for 24 h ($n=4$). Results were normalized to DMSO control and plotted as mean fold change.

assay to measure HO-1 in a 384 (or 1536) well format was developed to allow rapid, simple, accurate and relatively inexpensive high throughput screening for kidney toxicity, amenable to the Tox21 robotic platform for assessment of chemical-induced toxicity.[21,22]

HO-1 is ubiquitously expressed in unstressed cells at low levels but is highly induced in response to cell injury mediated by oxidative or proinflammatory stress, heavy metals, ischemia and hypoxia.[23,24] Its cytoprotective and anti-apoptotic properties are mediated by degradation of the pro-oxidant heme into iron, biliverdin and carbon monoxide via induction of p38 MAPK and PI3K/Akt signal transduction pathways.[25] In contrast, pronounced chemical or genetic inhibition of basal HO-1 levels is associated with increased cell death and tissue necrosis in models of Alzheimer's disease and aging.[26,27] These effects have partly been explained by a lowered antioxidative capacity[28] and cells being more susceptible to damaging agents during HO-1 inhibition,[29] a property that has been used to sensitize cells for cancer therapy.[30] Given that deregulation of HO-1 in HPTECs correlated well with the known toxic effects of the tested compounds in humans, changes in cellular HO-1 might indicate a cellular process to protect from further damage. HO-1 has previously been found to be upregulated in the urine of patients with AKI[18] or tubulointerstitial damage.[31] HO-1 expression was significantly upregulated in rat kidneys following tubular toxicity and in the human kidney-on-a-chip system following CdCl$_2$ exposure (Figure 4). Hence, we demonstrate the translatability of the 2D *in vitro* approach all the way to rats, MPSs and humans.

Two-dimensional monolayer cell culture for organs has advantages of being adaptable to high throughput applications such as small molecule discovery screening experiments,[32] 'omics'-based biomarker discovery (Figure 2) or pathway-based risk assessment screening.[33] However, despite the fact that HO-1 increase was more pronounced and reliable in primary human compared with immortalized kidney cells (Supplemental Figure 2C), the 2D system for kidney suffers from certain limitations. Those include: lack of estimating

toxicity of compounds that require metabolism and bioactivation by the liver, for example compounds such as acetaminophen, an analgesic with nephrotoxicity attributed to its hepatic metabolite N-acetyl-p-benzoquinone imine; lack of apical to basolateral polarity when cultured on a flat surface, which might not allow the uptake of certain antiviral drugs therefore misrepresenting its safety, for example OAT1 and OAT3, expressed at the basolateral membrane of proximal tubular epithelial cells mediating the uptake of antiviral agents tenofovir and acyclovir.[34,35] This lack of basolateral uptake of tenofovir may explain why we did not observe toxic effects in this study. Furthermore, the absence of immune or endothelial cells prevents the assessment of the nephrotoxic potential of immunologically active drugs. For example, the induction of pro-inflammatory cytokines via Toll-like receptors[36] is linked to the development of amphotericin B-induced nephrotoxicity in patients.[37] In our study the effects of amphotericin B on viability and expression of HO-1 in HPTECs was mild even at high doses, possibly because of a missing immune response in the cell culture system. Finally, the absence of flow might impact on the differentiation and function of the cells while preventing shear stress as well as the interactions with circulating molecules. To address some of these limitations the new organs-on-a-chip initiative aims at using microfluidic cell culture devices that contain continuously perfused chambers inhabited by living cells arranged to simulate tissue and organ-level physiology.[38] Although these types of *in vitro* systems are not amenable to high throughput screening, they may contribute additional orthogonal high content information about the mechanisms of kidney injury.

In summary, in this study we have taken a major step forward from the current approach of using immortalized cell lines and cell viability as an endpoint assay. The use of HO-1 as a translatable, sensitive and specific biomarker that is easy to combine with existing cytotoxicity assays, and the ability to measure HO-1 in 384-well plates using the HTRF assay provides an obvious advantage of scalability over other approaches.

CONCISE METHODS

Cells and Compounds
Primary HPTECs were purchased from Biopredic International (Rennes, France) and were cultured in supplemented DMEM/Hams-F12 with GlutaMAX medium. Human papillomavirus 16 (HPV-16) transformed kidney proximal tubule cells (HK-2) were purchased from ATCC (Manassas, VA) and cultured in keratinocyte serumfree medium. HPTECs were used in passages 3 and 4, HK-2 cells were used in passage 4. The 10 compounds of the discovery panel (Supplemental Table 1) were purchased from Sigma-Aldrich (Saint Louis, MO) and were used in a broad concentration range from 1.5 μM to 20 mM, reflecting their respective toxicity range *in vitro*. The compound library that was used as a validation panel contained 39 compounds (Supplemental Table 1) and was custom made from Enzo Life Sciences Inc. (Farmingdale, NY). Cells were cultivated for 3 d in 96 or 384-well plates until confluency and then incubated with either a vehicle control (0.5% DMSO) or toxic and nontoxic compounds in multiple concentrations ranging from 0.1 μM to 554 μM for 3, 6, 12 or 24 h using an automatic 384-well pin transfer system or manually. Cell viability based on ATP concentration was measured using the CellTiter-Glo Luminescent assay (Promega). KIM-1 protein was measured in cell lysate and supernatant using microsphere-based Luminex xMAP technology, as described previously.[16,39]

Live Cell Imaging and Measurement of Oxidative Stress (ROS) and Number of Dead Cells
Drug-induced changes in cell morphology, mitochondrial membrane potential, induction of oxidative stress and number of dead cells were quantified using live cell high content imaging. Briefly, 3 d after seeding in 384-well plates, HPTECs were co-incubated for 45 min with 0.5 μM Hoechst 33342 (Active Motif, Carlsbad, CA) to stain nuclei, 0.1 μM tetramethylrhodamine methyl ester (Molecular Probes, Eugene, OR) to measure changes in MMP, and 5 μM CellROX green reagent (Molecular Probes) to detect ROS. After washing off the fluorescent dyes, cells were incubated with 0.2 μM TOTO-3 iodine (Molecular Probes) to stain cells with impaired plasma membrane (dead cells), and treated with the compounds included in both the discovery panel (six concentrations; 1.5 μM to 20 mM) and the validation panel (six concentrations; 0.1 μM to 1000 μM), as well as mitochondrial toxicants (carbonyl cyanide m-chlorophenyl hydrazone, oligomycin A) and live cell images were taken at 3, 6, 12 and 24 h. Experiments were performed in four biologic replicates with duplicate wells on each plate.

Gene Expression Profiling Using L1000 Platform
HPTECs cultured in 96-well plates were treated with the 10 toxic and nontoxic compounds in the discovery panel (Supplemental Table 1) in six concentrations (1.6 μM to 20 mM) for 3, 6, 12 and 24 h, and lysed with 100 μl of TCL buffer (Qiagen). Cell lysates were added to the well of a TurboCapture 384 plate to perform mRNA isolation and cDNA synthesis in the same well (TurboCapture 384 mRNA kit; Qiagen). High throughput gene expression analysis is based on the measurement of about 1000 transcripts as described previously.[40] Replicates were averaged and values were z-scored across all data. For each pair of gene and drug, Spearman's correlation $Rho_1, ..., Rho_4$ between the gene expression and the six doses across all four time points ($t_1, ..., t_4$) was calculated. The sum of squares of correlation $|Rho|^2 = \Sigma\ Rho_i^2$ for $i=1, ..., 4$ if $Rho_i > 0$ was compared with values of $|Rho|^2$ obtained from the correlation of six random values. The comparison with 5,000,000 random values of $|Rho|^2$ yields an empirical *P* value. A FDR value was obtained using the Benjamini and Hochberg procedure and gene expression was considered to be significantly positively correlated with drug if FDR<0.01.

Structural Characterization and HO-1 Measurement by Immunofluorescence Staining
Primary antibodies used were mouse anti-zonula occludens-1 (Invitrogen), mouse anti–N-cadherin (BD Transduction), mouse anti-CK18 (CK18; Abcam, Inc., Cambridge, MA), rat anti–E-cadherin (Abcam, Inc.), and mouse anti–HO-1 (BD Transduction). Donkey anti-rat FITC-conjugated antibodies were obtained from Jackson ImmunoResearch, and Alexa Fluor 488 donkey anti-mouse was from Invitrogen. HPTECs were grown on 8-well glass chamber slides

or 384-well plates, fixed in 4% paraformaldehyde or methanol/acetone (1:1), permeabilized with 0.1% Triton X-100, blocked with 5% donkey serum and incubated with respective primary antibody overnight at 4°C. Four replicates were conducted as two replicates on each of two separate days.

Quantification of HO-1 levels and the total number of cells was performed in 384-well plates using immunofluorescence after incubation with eight concentrations (0.1 μM to 554 μM) of each of the 39 compounds included in the validation panel for 24 h. Images (10×, four areas per well) were segmented and quantified using Meta-Express 2.0 (Molecular Devices). The cell scoring module was used to count individual cells (total cells readout) and quantify the level of HO-1 in each cell (% positive cells readout). The readouts for the eight negative vehicle control wells on each 384-well plate were averaged to obtain per-plate baseline values for cell count and percentage of HO-1-positive cells. All noncontrol readouts were divided by the appropriate baseline values to obtain normalized values for cell viability (based on cell number) and fold change in HO-1 expression.

HO-1 Measurement by ELISA and HTRF
ELISA
HPTECs or HK-2 cells were lysed in RIPA buffer and the amount of HO-1 in the cell lysates was quantified by DuoSet IC human total HO-1/HMOX1 ELISA kit purchased from R&D Systems Inc. (Minneapolis, MN).

HTRF
The development and optimization process examined best antibody pair analysis, reaction volumes, buffer compositions, cell lysate concentrations and antibody reaction concentrations, and incubation times, with the aim of obtaining a FRET signal following cytotoxicity in HPTECs. A recombinant human HO-1 protein (Abcam, Inc.) was used to generate a standard curve. The best antibody pair showing high Delta F (%) signal between positive and negative lysates was rabbit monoclonal HO-1-antibody (Cell Signaling Technology) labeled with europium cryptate (k) and a d2-conjugated rabbit polyclonal anti HO-1 antibody (Cell Signaling Technology). To detect HO-1 in cell lysates of HPTECs exposed to several compounds, cells were lysed with either 50 μl of Cisbio Lysis Buffer 1 (LB1; Cisbio Bioassays, Bedford, MA) supplemented with 1× protease inhibitor cocktail (96-well) or 10 μl of 4× LB1 (384-well) and stored at –80°C until use. The HTRF emission at 620 nm and 665 nm wavelengths were measured on the Molecular Devices SpectraMax Paradigm using the standard HTRF protocol after 4 h of incubation. Emission at 620 nm is used as internal reference, while emission at 655 nm is proportional to the amount of HO-1. Data are presented as percentages of Delta F [(665/620 ratio–background ratio)/background ratio].

Semiquantitative and Real-Time PCR
Total RNA was isolated, transcribed into cDNA and quantitative or semiquantitative PCR was performed using primers for specific genes listed in Supplemental Table 2.

Transport Activity and Enzymatic Assays
HPTECs were seeded onto collagen IV-coated 6.5 mm, 0.4 μM pore size 24-well Transwell inserts (Corning Life Science) at a density of

$2.5×10^4$ cells/well. Cells were incubated with either apically or basolaterally applied [^{14}C]-sucrose at a concentration of 100 nCi/ml for up to 60 min. An aliquot of 50 μl was removed from the apical and basolateral chamber after 7, 15, 30, and 60 min and the flux was measured using a Beckman scintillation counter. Time and dose-dependent uptake of glucose was measured after incubation of cells with 100, 200, or 500 μM of the fluorescent substrate 2-(N-(7-nitrobenz-2-oxa-1,3-diazol-4-yl)amino)-2-deoxyglucose (2-NBDG) over the course of 120 min in 96-well plates.[41] Competitive inhibition of SGLT activity was determined in transwell plates after incubation with 250 μM 2-NBDG for 1 h in the presence or absence of 1000 μM phlorizin (SGLT inhibitor) in Na+ and Na+ free buffers. Inhibition of Na+-independent, facilitative transporter activity (GLUT) was shown after pretreatment of HPTECs for 10 min with 50 mM cytochalasin B (SGLT inhibitor) followed by 1 h incubation with 250 μM 2-NBDG in Na+ and Na+ free buffers. The fluorescence intensity of 2-NBDG was measured at excitation and emission wavelengths of 485 nm and 528 nm, respectively, using a Synergy ^{1}H microplate reader (BioTek Instruments, Inc.). Efflux of rhodamine 123 across cell monolayers was measured by incubation of the cells with 0.5 μg/ml substrate for 2 h. Cells were trypsinized, and incubated in rhodamine free media for 0, 7, 15, 30 and 60 min. Rhodamine fluorescence intensity was quantified at 520nm using a flow cytometer (BD Biosciences). Experiments were done in triplicate and were repeated three times. Mean fluorescence intensity was calculated using FlowJo software and plotted. γ-Glutamyl transferase activity was determined by a colorimetric assay from Biovision (Milpitas, CA) in cells treated with 25 or 50 μM $CdCl_2$ for 24 h and glutathione levels were measured with GSH-Glo assay (Promega) in cells treated with 10 or 50 μM $CdCl_2$ for 6, 12 and 24 h.

Comparison of HO-1 as Biomarker for Kidney Injury with Known Cell Viability/Cell Death Assays
To compare the predictive performance of HO-1 immunofluorescence staining with established assays of cell toxicity, we first reduced the datasets so that each of the 39 compounds in the validation panel (measured in six to eight different concentrations between 0.1 and 1000 μM) had just one assigned output value per assay. This single value was determined for each of the four assays (HO-1, cell number, ATP concentration, and dead cell number) as the maximal significant deregulation compared with control that could be observed at any given concentration of a drug.

We calculated the AUC-ROC both for proximal tubule toxic drugs only and nephrotoxicants including indirectly acting compounds. To determine for each assay where sensitivity and specificity are maximal, the Youden index was calculated as sensitivity (%)+specificity (%)–100. Applying this cutoff for each assay, sensitivity was calculated by dividing the number of true positive toxicants by the number of total toxicants in the validation panel. Specificity was calculated by dividing the number of true negative nontoxicants by the number of total nontoxicants in the set. The positive predictive value is defined as the ratio of true positive toxicants to all compounds identified as toxic and the negative predictive value is calculated as the ratio of true negative nontoxicants to all compounds identified as nontoxic. Chi-squared test statistic and corresponding P value were calculated to

describe the goodness of fit of the observed distribution (measured results in the respective assays) to the theoretical one (toxic or non-toxic). Improvement of predictivity via combination of cell death/viability assays with HO-1 was calculated using logistic regression. A combined output was calculated as $\alpha_0 + \alpha_1 *$value assay 1(HO-1) $+\alpha_2 *$value assay 2. The final AUC-ROC were calculated using the combined output values both for proximal tubule toxic drugs only and when indirect nephrotoxicants are included.

To include dose-response data into the analysis of HO-1 performance, we used the cell viability data (based on cell number) to compute the IC_{25} (concentration that kills 25% of the cells), and the HO-1 fold change data to compute C_{HO-1} (concentration at which HO-1 induction was 2 SD above or below the baseline in the log domain). To obtain IC_{25} values from cell viability data, replicates were combined by averaging and the resulting values were fit to four-parameter logistic curves using the L-BFGS-B nonlinear optimization algorithm implemented in Python's SciPy library. The IC_{25} was computed by interpolating each fitted viability dose-response curve to find the concentration where the normalized cell viability was 0.75. C_{HO-1} values were computed from the HO-1 fold change data by first discarding data points for concentrations above the computed IC_{25} for each drug (toxicity effects and low total cell numbers rendered the data inconsistent and noisy) and then applying the same logistic curve fitting procedure described above on the remaining data. The C_{HO-1} was computed by interpolating each fitted HO-1 expression dose-response curve to find the concentration where HO-1 expression exceeded the baseline by plus or minus two times the SD of all negative controls, calculated in the log domain (*i.e.*, the geometric mean multiplied or divided by the geometric SD squared). We flagged each compound as +*TOX* if it achieved at least 25% toxicity (*i.e.*, the E_{max} for the viability dose-response curve was 0.75 or lower) and thus had a defined IC_{25}, or –*TOX* if it did not in which case we set its IC_{25} to 1000 μM. Likewise, we used +*HO-1* to indicate compounds that showed significant HO-1 induction and thus a defined C_{HO-1}, and –*HO-1* for those that did not in which case we set the C_{HO-1} to 1000 μM. The combination of these descriptors defines four response categories: +TOX/+HO-1, –TOX/–HO-1, –TOX/+HO-1 and +TOX/–HO-1.

Evaluation of HO-1 Expression Using *In Vivo* Toxicogenomic Databases

To determine the gene expression profile of HO-1 (*Hmox-1*) following kidney toxicity *in vivo*, two public toxicogenomics datasets: Drug-Matrix (of the National Toxicology Program; https://ntp.niehs.nih.gov/drugmatrix/index.html) and TG-GATES (of the National Institute of Biomedical Innovation; http://toxico.nibio.go.jp/english/index.html) that track kidney gene expression using Affymetrix 230 2.0 microarrays were mined. Prior to the analysis described below, kidney microarray datasets were normalized using the RMA algorithm[42,43] implemented in GeneSpring GX 12.6 (Agilent Technologies, Palo Alto, CA). The Drug-Matrix and TG-GATES kidney datasets are composed of 1410 and 3728 microarrays, respectively. The DrugMatrix and TG-GATES gene expression data are available through the GEO (Series ID: GSE57811) and ArrayExpress databases (E-MTAB-800), respectively. Association between kidney tubule necrosis and normalized expression of *Hmox1* or *Havrc1* in rat kidney was determined using the Welch *t* test (also known

as an unequal variances *t* test) implemented in GeneSpring GX 12.6. Association between *Hmox1* expression and expression of validated kidney toxicity transcriptional biomarkers was performed in Microsoft Excel (Microsoft Corp., Redmond, WA) using the regression statistical function.

Evaluation of HO-1 Expression in a 3D Human Kidney MPS

Cell Isolation and Culture

Human kidney tissue was obtained from a healthy mass after surgery due to diagnosis of renal carcinoma at the University of Washington Medical Center. The University of Washington Institutional Review Board approved human subjects protocol. Tissue for kidney tubule epithelial cell isolation was stored at 4°C in HBSS buffer containing Pen-Strep and was processed within 24 h as previously described.[17] Primary renal epithelial cells were cultured and grown to confluency in approximately 10 d under normal static conditions.

Cell Seeding in Nortis Device

The kidney tubule MPS consists of a tubule embedded in a collagen I matrix. Physical dimensions of the tubule are a length of approximately 6 mm, with an internal diameter of 120 μM and volume of 70 nl. Each tubule contains approximately 5000 primary proximal tubular epithelial cells. The proximal tubular epithelial cells form a patent confluent tubule that is self-assembling with tight junctions and expression of epithelial markers, including markers of polarization (Weber *et al.*, manuscript in preparation). The Nortis MPS devices were first filled with extracellular matrix of rat tail collagen type I (Ibidi Inc., Verona, WI) at 6mg/ml at 4°C. The devices were left at 4°C for 30 min and then room temperature overnight. To seed the MPS devices, 3–4 μl of cell suspension was injected into the lumen of each device. Cells were allowed to recover from trypsin digestion and adhere for 24 h before initiating flow at 0.5 μl/min. The integrity of the tubule cell structure was assessed grossly by light microscopy on a weekly basis and viability at 4 wks was determined using a LIVE/DEAD Viability/Cytotoxicity kit (Invitrogen, Carlsbad, CA).

Assessment of CdCl$_2$-Induced Nephrotoxicity

MPS devices with approximately 100% tubule confluency after 14+ d in culture were used. Cadmium chloride (Sigma-Aldrich) was flowed through the devices at a final concentration of 25 μM CdCl2 while control devices were flowed with normal DMEM-F12 media (0 μM CdCl2) for 48 h. At the termination of the experiment, HPTECS in Nortis devices were fixed, permeabilized, blocked and immunofluorescence staining for HO-1 and KIM-1 was performed using respective primary and secondary antibodies: HO-1 (rabbit 1:100; Abcam, Inc.) and KIM-1 (mouse 1:100; R&D Systems, Minneapolis, MN) and goat anti-rabbit or goat anti-mouse (1:1000; Abcam, Inc.) secondary antibodies. Fluorescence images were acquired on Nikon Eclipse Ti-S.

Statistics

Unless otherwise indicated, data are presented as mean±SEM. Statistical difference ($P<0.05$) as calculated by Student's *t* test. Multiple group comparison was conducted by ANOVA followed by Dunnett's *post hoc* test. $P<0.05$ was considered significant and represented by *

as compared with corresponding controls. All graphs were generated using GraphPad Prism (GraphPad, Inc., La Jolla, CA), MATLAB (MathWorks, Natick, MA) or Matplotlib (open source/J.D. Hunter). Receiver-operator characteristic curves and other statistical parameters like chi-squared, *P* value, and sensitivity/specificity, were calculated using GraphPad Prism (GraphPad, Inc.). Logistic regression parameters of the combined assays were calculated using StatPages (statpages.org/logistic.html, John C. Pezzullo, Washington, DC).

DISCLOSURES

None.

REFERENCES

1. Bonventre JV, Vaidya VS, Schmouder R, Feig P, Dieterle F: Next-generation biomarkers for detecting kidney toxicity. *Nat Biotechnol* 28: 436–440, 2010
2. Soderland P, Lovekar S, Weiner DE, Brooks DR, Kaufman JS: Chronic kidney disease associated with environmental toxins and exposures. *Adv Chronic Kidney Dis* 17: 254–264, 2010
3. Hartung T: Toxicology for the twenty-first century. *Nature* 460: 208–212, 2009
4. Fuchs TC, Hewitt P: Biomarkers for drug-induced renal damage and nephrotoxicity – an overview for applied toxicology. *AAPS J* 13: 615–631, 2011
5. Sun H, Xia M, Austin CP, Huang R: Paradigm shift in toxicity testing and modeling. *AAPS J* 14: 473–480, 2012
6. Shukla SJ, Huang R, Austin CP, Xia M: The future of toxicity testing: a focus on in vitro methods using a quantitative high-throughput screening platform. *Drug Discov Today* 15: 997–1007, 2010
7. Ryan MJ, Johnson G, Kirk J, Fuerstenberg SM, Zager RA, Torok-Storb B: HK-2: an immortalized proximal tubule epithelial cell line from normal adult human kidney. *Kidney Int* 45: 48–57, 1994
8. Gstraunthaler G, Pfaller W, Kotanko P: Biochemical characterization of renal epithelial cell cultures (LLC-PK1 and MDCK). *Am J Physiol* 248: F536–F544, 1985
9. Jenkinson SE, Chung GW, van Loon E, Bakar NS, Dalzell AM, Brown CD: The limitations of renal epithelial cell line HK-2 as a model of drug transporter expression and function in the proximal tubule. *Pflugers Arch* 464: 601–611, 2012
10. Li Y, Oo ZY, Chang SY, Huang P, Eng KG, Zeng JL, Kaestli AJ, Gopalan B, Kandasamy K, Tasnim F, Zink D: An in vitro method for the prediction of renal proximal tubular toxicity in humans. *Toxicol Res (Camb)* 2: 352–365, 2013
11. Perazella MA: Renal vulnerability to drug toxicity. *Clin J Am Soc Nephrol* 4: 1275–1283, 2009
12. Li Y, Kandasamy K, Chuah JK, Lam YN, Toh WS, Oo ZY, Zink D: Identification of nephrotoxic compounds with embryonic stem-cell-derived human renal proximal tubular-like cells. *Mol Pharm* 11: 1982–1990, 2014
13. Lash LH, Putt DA, Cai H: Membrane transport function in primary cultures of human proximal tubular cells. *Toxicology* 228: 200–218, 2006
14. Lash LH, Putt DA, Cai H: Drug metabolism enzyme expression and activity in primary cultures of human proximal tubular cells. *Toxicology* 244: 56–65, 2008
15. Lamb J: The Connectivity Map: a new tool for biomedical research. *Nat Rev Cancer* 7: 54–60, 2007
16. Vaidya VS, Ozer JS, Dieterle F, Collings FB, Ramirez V, Troth S, Muniappa N, Thudium D, Gerhold D, Holder DJ, Bobadilla NA, Marrer E, Perentes E, Cordier A, Vonderscher J, Maurer G, Goering PL, Sistare FD, Bonventre JV: Kidney injury molecule-1 outperforms traditional biomarkers of kidney injury in preclinical biomarker qualification studies. *Nat Biotechnol* 28: 478–485, 2010
17. Kelly EJ, Wang Z, Voellinger JL, Yeung CK, Shen DD, Thummel KE, Zheng Y, Ligresti G, Eaton DL, Muczynski KA, Duffield JS, Neumann T, Tourovskaia A, Fauver M, Kramer G, Asp E, Himmelfarb J: Innovations in preclinical biology: ex vivo engineering of a human kidney tissue microperfusion system. *Stem Cell Res Ther* 4[Suppl 1]: S17, 2013
18. Zager RA, Johnson AC, Becker K: Plasma and urinary heme oxygenase-1 in AKI. *J Am Soc Nephrol* 23: 1048–1057, 2012
19. Astashkina AI, Mann BK, Prestwich GD, Grainger DW: A 3D organoid kidney culture model engineered for high-throughput nephrotoxicity assays. *Biomaterials* 33: 4700–4711, 2012
20. Huang JX, Blaskovich MA, Cooper MA: Cell- and biomarker-based assays for predicting nephrotoxicity. *Expert Opin Drug Metab Toxicol* 10: 1621–1635, 2014
21. Attene-Ramos MS, Miller N, Huang R, Michael S, Itkin M, Kavlock RJ, Austin CP, Shinn P, Simeonov A, Tice RR, Xia M: The Tox21 robotic platform for the assessment of environmental chemicals – from vision to reality. *Drug Discov Today* 18: 716–723, 2013
22. Tice RR, Austin CP, Kavlock RJ, Bucher JR: Improving the human hazard characterization of chemicals: a Tox21 update. *Environ Health Perspect* 121: 756–765, 2013
23. Agarwal A, Bolisetty S: Adaptive responses to tissue injury: role of heme oxygenase-1. *Trans Am Clin Climatol Assoc* 124: 111–122, 2013
24. Nath KA: Heme oxygenase-1 and acute kidney injury. *Curr Opin Nephrol Hypertens* 23: 17–24, 2014
25. Gozzelino R, Jeney V, Soares MP: Mechanisms of cell protection by heme oxygenase-1. *Annu Rev Pharmacol Toxicol* 50: 323–354, 2010
26. Takahashi M, Doré S, Ferris CD, Tomita T, Sawa A, Wolosker H, Borchelt DR, Iwatsubo T, Kim SH, Thinakaran G, Sisodia SS, Snyder SH: Amyloid precursor proteins inhibit heme oxygenase activity and augment neurotoxicity in Alzheimer's disease. *Neuron* 28: 461–473, 2000
27. Harder Y, Amon M, Georgi M, Scheuer C, Schramm R, Rücker M, Pittet B, Erni D, Menger MD: Aging is associated with an increased susceptibility to ischaemic necrosis due to microvascular perfusion failure but not a reduction in ischaemic tolerance. *Clin Sci (Lond)* 112: 429–440, 2007
28. Regehly M, Greish K, Rancan F, Maeda H, Böhm F, Röder B: Water-soluble polymer conjugates of ZnPP for photodynamic tumor therapy. *Bioconjug Chem* 18: 494–499, 2007
29. Berberat PO, Dambrauskas Z, Gulbinas A, Giese T, Giese N, Kunzli B, Autschbach F, Meuer S, Buchler MW, Friess H: Inhibition of heme

oxygenase-1 increases responsiveness of pancreatic cancer cells to anticancer treatment. *Clinical cancer research: an official journal of the American Association for Cancer Research*, 11: 3790–3798, 2005.

30. Abraham NG, Kappas A: Pharmacological and clinical aspects of heme oxygenase. *Pharmacol Rev* 60: 79–127, 2008

31. Yokoyama T, Shimizu M, Ohta K, Yuno T, Okajima M, Wada T, Toma T, Koizumi S, Yachie A: Urinary heme oxygenase-1 as a sensitive indicator of tubulointerstitial inflammatory damage in various renal diseases. *Am J Nephrol* 33: 414–420, 2011

32. Shan J, Schwartz RE, Ross NT, Logan DJ, Thomas D, Duncan SA, North TE, Goessling W, Carpenter AE, Bhatia SN: Identification of small molecules for human hepatocyte expansion and iPS differentiation. *Nat Chem Biol* 9: 514–520, 2013

33. Huang R, Xia M, Cho MH, Sakamuru S, Shinn P, Houck KA, Dix DJ, Judson RS, Witt KL, Kavlock RJ, Tice RR, Austin CP: Chemical genomics profiling of environmental chemical modulation of human nuclear receptors. *Environ Health Perspect* 119: 1142–1148, 2011

34. Cihlar T, Ho ES, Lin DC, Mulato AS: Human renal organic anion transporter 1 (hOAT1) and its role in the nephrotoxicity of antiviral nucleotide analogs. *Nucleosides Nucleotides Nucleic Acids* 20: 641–648, 2001

35. Takeda M, Khamdang S, Narikawa S, Kimura H, Kobayashi Y, Yamamoto T, Cha SH, Sekine T, Endou H: Human organic anion transporters and human organic cation transporters mediate renal antiviral transport. *J Pharmacol Exp Ther* 300: 918–924, 2002

36. Sau K, Mambula SS, Latz E, Henneke P, Golenbock DT, Levitz SM: The antifungal drug amphotericin B promotes inflammatory cytokine release by a Toll-like receptor- and CD14-dependent mechanism. *J Biol Chem* 278: 37561–37568, 2003

37. Chai LY, Netea MG, Tai BC, Khin LW, Vonk AG, Teo BW, Schlamm HT, Herbrecht R, Donnelly JP, Troke PF, Kullberg BJ: An elevated pro-inflammatory cytokine response is linked to development of amphotericin B-induced nephrotoxicity. *J Antimicrob Chemother* 68: 1655–1659, 2013

38. Bhatia SN, Ingber DE: Microfluidic organs-on-chips. *Nat Biotechnol* 32: 760–772, 2014

39. Vaidya VS, Waikar SS, Ferguson MA, Collings FB, Sunderland K, Gioules C, Bradwin G, Matsouaka R, Betensky RA, Curhan GC, Bonventre JV: Urinary biomarkers for sensitive and specific detection of acute kidney injury in humans. *Clin Transl Sci* 1: 200–208, 2008

40. Peck D, Crawford ED, Ross KN, Stegmaier K, Golub TR, Lamb J: A method for high-throughput gene expression signature analysis. *Genome Biol* 7: R61, 2006

41. Blodgett AB, Kothinti RK, Kamyshko I, Petering DH, Kumar S, Tabatabai NM: A fluorescence method for measurement of glucose transport in kidney cells. *Diabetes Technol Ther* 13: 743–751, 2011

42. Irizarry RA, Bolstad BM, Collin F, Cope LM, Hobbs B, Speed TP: Summaries of Affymetrix GeneChip probe level data. *Nucleic Acids Res* 31: e15, 2003

43. Irizarry RA, Hobbs B, Collin F, Beazer-Barclay YD, Antonellis KJ, Scherf U, Speed TP: Exploration, normalization, and summaries of high density oligonucleotide array probe level data. *Biostatistics* 4: 249–264, 2003